Vol. 2 No. 5 (2024)

Spectrum of Engineering Sciences

SPECTRUM OF ENGINEERING SCIENCES

Online ISSN
3007-3138
Print ISSN
3007-312X

Synthesis and Characterization of Magnesium Doped Bismuth Phosphate Nanomaterial's for Antifungal and Antibacterial Packaging

Iqra Batool[1]
Faculty of Sciences , The Superior University Lahore, Pakistan
Aneela Din Muhammad[2]
Faculty of Sciences, The Superior University Lahore, Pakistan
Dr. Kanwal Akhtar[3*]
Faculty of Sciences, The Superior University, Lahore, Pakistan
Yasir Javed[4]
Department of Physics, University of Agriculture, Faisalabad, Pakistan
Fayyaz Ahmad[5]
Faculty of Sciences , The Superior University Lahore, Pakistan
Zeeshan Mahmood[6]
Faculty of Sciences, The Superior University Lahore, Pakistan

Abstract

Magnesium-doped bismuth phosphate (Mg-$BiPO_4$) nanoparticles were synthesized using the sol-gel method, offering a cost-effective and scalable approach to obtain highly crystalline and uniform nanomaterials. The optical and compositional properties of the synthesized materials were characterized by UV-Visible spectroscopy and Fourier-transform infrared spectroscopy (FTIR). Vibrational bands of bismuth phosphate were detected by Fourier transform infrared spectroscopy. UV-visible spectroscopy shows decreased optical band gap. Using disk diffusion and minimum inhibitory concentration (MIC) experiments, the antifungal activity of Mg-$BiPO_4$ was assessed against common pathogenic fungi, such

Spectrum of Engineering Sciences
Online ISSN
3007-3138
Print ISSN
3007-312X
SPECTRUM OF ENGINEERING SCIENCES

as Aspergillus niger. The results showed that bismuth phosphate's antifungal effectiveness was considerably increased by magnesium doping, most likely as a result of increased reactive oxygen species (ROS) production and surface activity. With lower MIC values than undoped bismuth phosphate, the material demonstrated broad-spectrum antifungal activity, suggest it as useful antifungal agent. The antimicrobial activity of Mg-$BiPO_4$ was evaluated against Gram-positive and Gram-negative bacteria, as well as fungi, using the sol-gel method. Mg doping significantly enhanced the antimicrobial efficacy of bismuth phosphate, attributed to the synergistic effects of magnesium ions and bismuth species. Zone of inhibition studies revealed superior performance compared to undoped $BiPO_4$, indicating potential applications in antimicrobial coatings and biomedical devices.

Keywords: Bismuth phosphate, Compositional properties, Antimicrobial, FTIR, UV-visible, Sol Gel

Introduction

Antimicrobial resistance is accelerated by the repetitive or improper use of antibiotics in human and animals. New antimicrobial drugs are desperately needed to combat these microorganisms. Gram-negative bacteria's are particularly significant among these diseases due to their multi-antibiotic resistance. Might be the result of these bacteria's capacity to develop novel defense mechanisms against antibiotic therapy. As a result, the scientific community now uses the list of priority diseases as a guide to choose where to concentrate efforts in order to control the next epidemic danger. Among other things, WHO's antimicrobial resistance reduction initiatives seek to reduce infection rates, increase knowledge via research and monitoring,

Spectrum of Engineering Sciences
Online ISSN
3007-3138
Print ISSN
3007-312X
SPECTRUM OF ENGINEERING SCIENCES

enhance awareness and comprehension of antimicrobial resistance, and maximize the use of antimicrobial drugs (Lin et al., 2013). Many materials with antibacterial potential have been investigated recently, particularly against certain bacterial strains, in order for research to quickly address these pressing public health requirements. Antimicrobial resistance is a complicated process that is based on both acquired (the bacterial adaptive ability to acquire new genetic material that increases the likelihood of bacterial survival despite antibiotic therapy) and intrinsic (the existing genetic material exhibits novel behaviors to avoid the action of the antibiotic) characteristics (Murimadugula et al., 2024).

Multi-antibiotic resistance in many bacterial species (such as Enterococcus species, Staphylococcus species, Streptococcus species, and Listeria species) results from an interspecies transfer of resistance mediated by plasmids. The effectiveness of several metal nanoparticles, including copper, titanium, bismuth, and silver, as well as metal oxide particles, including zinc oxide nanoparticles, titanium oxides, and bismuth oxides, in terms of antibacterial activity has been investigated over time. Large surface-to-volume ratios and distinct structural forms and sizes of inorganic nanoparticles that permit contact with bacteria are among their benefits in terms of antibacterial potential (Ianăși et al., 2023). These features of nanoparticles allow them to lower the likelihood of antibacterial resistance since they constitute the primary difference in interaction when compared to microbial agents. For instance, bismuth oxide nanoparticles' crystalline structure. Since nanoparticles can be made in a range of sizes and shapes that prevent bacteria from adapting to them and because they can form free metal ions that have a biocidal effect, one of their most

Spectrum of Engineering Sciences
SPECTRUM OF ENGINEERING SCIENCES
Online ISSN
3007-3138
Print ISSN
3007-312X

significant characteristics is that they lower the likelihood of developing antimicrobial resistance (Nagay et al., 2019). Numerous techniques, including sol-gel procedures, wet chemical synthesis, solution combustion, and metal vapour oxidative deposition, evaporation, thermal oxidation, and pulsed laser ablation in liquids, can be used to produce bismuth phosphate (Pancotti et al., 2024).

Materials based on bismuth phosphate have several uses, including in optical engineering, microelectronics, as a photocatalyst, as a surface disinfectant in hospitals and the food business, in the manufacturing of pharmaceuticals, and as a necessary derivative in the glass and ceramics industries, in medicine and as an agent in anticancer therapy. It has been discovered that the manufacturing method affects the size and shape of manufactured bismuth oxide nanoparticles. In light of this, materials based on bismuth phosphates have been created in this paper using the same synthesis method. It was discovered that the morphology of the produced particles varies, and this has a major effect on the rate at which microbial growth is inhibited. In order to retrieve these metal ions from spent solutions, doping inorganic metal ion materials is a popular choice. These metal ions may then "adapt" and enhance the characteristics of the materials on which they have been adsorbed, especially to counteract antibiotic resistance (Ashfaq et al., 2023). According to a number of studies, the antibacterial activity of metal ions is caused by their positive charge, which enables electrostatic interaction between the positive charge of the nanoparticles and the negative charge on the bacterial cell membrane. The preparation of three distinct series of bismuth phosphate nanocomposites was the goal of the current effort. Using bismuth carbonate as the precursor, the

Spectrum of Engineering Sciences
SPECTRUM OF ENGINEERING SCIENCES
Online ISSN
3007-3138
Print ISSN
3007-312X

required material was created by sol-gel synthesis in the first series, yielding white foam. Additionally, all of the nanocomposite materials from the second and third series—many of which had a gel structure—were made utilizing the bismuth phosphate foam that was acquired in the first series (Meng et al., 2023).

Global health is facing serious challenges due to the rise in drug-resistant fungal strains and the prevalence of fungal infections. Although traditional antifungal agents are somewhat effective, they frequently have drawbacks like toxicity, high cost, and decreased efficacy against resistant strains (Niemirowicz et al., 2017). These issues have sparked interest in creating novel materials with improved antifungal properties, especially in the fields of nanotechnology and doped compounds. Bismuth-based materials have attracted a lot of attention recently because of their unique physicochemical properties, such as antimicrobial activity, biocompatibility, and environmental stability. Of these, bismuth phosphate ($BiPO_4$) is a promising candidate because of its high thermal stability, non-toxicity, and potential uses in photocatalysis, biomedical fields, and environmental remediation (Wang et al., 2014). This work aims to bridge the gap between material science and biomedical applications by synthesizing Mg-$BiPO_4$ using a controlled doping method, characterizing its physicochemical properties, and evaluating its activity against fungal strains. The goal of this study is to investigate the antifungal activity of Mg-doped bismuth phosphate and evaluate its potential as an effective antifungal material (Asghari et al., 2016). The results of this research could lead to the development of new, effective, and sustainable antifungal solutions. Doped bismuth phosphate is investigated in this work and demonstrated to have strong

Spectrum of Engineering Sciences
SPECTRUM OF ENGINEERING SCIENCES
Online ISSN
3007-3138
Print ISSN
3007-312X

antibacterial qualities against S. aureus, P. aeruginosa, and E. coli (Díez-Pascual, 2018).

Materials and Methods

Materials

Bismuth nitrate (Bi $(NO_3)_3$ $.5H_2O$), Potassium phosphate (K_2HPO_4), Magnesium hydrate hexahydrate ($MgCl_2$. $6H_2O$) and ethylene glycol were purchased from DEAJUNG Korea. Nitric acid and distilled water were purchased from Sigma Aldrich. All chemicals were of analytical grade and used without further purification.

Synthesis of Mg-doped Bismuth Phosphate

Mg-doped bismuth phosphate nanoparticles were prepared by using sol-gel method. Chemicals required for prepared Mg-doped bismuth phosphate nanomaterials were Bismuth nitrate (Bi $(NO_3)_3.5H_2O$ + Potassium phosphate (K_2HPO_4) is 0.85g and 15% of Magnesium hydrate hexahydrate ($MgCl_2$. $6H_2O$). To prepare Mg-doped bismuth phosphate we added 132ml of distilled water and 66ml of ethalene glycol in 250ml beaker. After that we added bismuth nitrate (9.70 g/mol) in beaker and stirred for 1 hour. In another beaker of 250ml were added potassium phosphate (3.48) and distilled water of 200ml and stirred for 30min. This solution added drop wise in firstly prepared solution and stirred for 15 minutes, then we left this solution for 15min. After that 4ml of nitric acid added in this solution and placed overnight. Next day, the solution was washed with distilled water by centrifuge machine to remove impurities. In this way precipitates of Mg-doped bismuth phosphate were obtained. Mg-doped $BiPO_4$ added to crucible and placed overnight dry. After grinding, the sample was added to falcon tube.

Spectrum of Engineering Sciences
SPECTRUM OF ENGINEERING SCIENCES
Online ISSN
3007-3138
Print ISSN
3007-312X

Characterization Tools for Synthesized Material

Fourier Transform Infrared Spectroscopy (FTIR) was used for analysis of vibrational modes and bonding, confirmed the incorporation of Mg into the lattice structure. FTIR spectrum was verified through Bruker Alpha spectrophotometer (Kumar, Vijayalakshmi, et al., 2022). The optical properties were premeditated through T80 UV/Vis spectrophotometer PG instruments LT9. UV-visible spectroscopy was used for analysis of the optical properties and determination of band gap energy of Mg-doped $BiPO_4$. Through UV-Visible optical absorption was accessed as well as calculated the band gap energy to evaluate possible changes in optical characteristics brought on by magnesium doping (Damodaraiah et al., 2017).

Antimicrobial Activity

The Disc Diffusion technique was used to examine the antibacterial activity of mg-doped bismuth phosphate nanoparticles against gram-positive S. aureus and gram-negative E. coli. Bacterial cultures were cultivated overnight and serially diluted to 1 106 CFU/mL for this evaluation. A sterile brush was then used to spread 50u of the bacterial solution onto Muller Hinton Agar plates, and the plates were allowed to dry for 30 minutes. After that, 5mm sterile filter paper discs were filled with 10ug/mL of NP's suspension, and the medium was carefully placed over the plates. The appositive control was ciprofloxacin. For 24 hours, these plates were incubated at 37°C. The antibacterial capability of nanomaterials was evaluated by measuring the zone of inhibition (ZOI) in millimeters. The experiment was conducted three times in order to obtain the readings. The inhibitory zone was evaluated using microtiter assays. Twenty microliters of bacterial strains and

Spectrum of Engineering Sciences
Online ISSN
3007-3138
Print ISSN
3007-312X
SPECTRUM OF ENGINEERING SCIENCES

100 microliters of material were placed in ninety-six well-flat bottom culture plates. The suppression of E. coli and S. aureus bacteria was investigated. Phosphate buffer saline served as the negative control and ciprofloxacin as the positive control (Biemer, 1973).

For 24 hours, the setup was incubated at 37°C while being covered aerobically. The samples from each well were then taken out and cleaned three times using sterile phosphate buffer (220 µL) with a pH of 7.2 in each well. With 220 µL of 99% methanol, the stability of the remaining bacteria was noted. Following drying, the plates were dyed for five minutes using 220 µL of crystal violet (7%) solution. Distilled water was used to wipe away the excess discoloration. Following plate air drying, 220 µL of 33% (v/v) glacial acetic acid was used to resolubilized each dye-containing well. The optical density of every well was measured at 630 nm using a micro-plate reader (Bakht et al., 2011). The percentage of bacterial growth inhibition was calculated using the following formula.

$$\%\, inhibition = 100 - \left[\frac{OD\ sample_{360}}{OD\ control_{360}} \times 100\right]$$

Results and Discussion

Characterization of Synthesized Material

UV-visible absorption spectrum of Mg-doped Bismuth Phosphate is shown in the Figure 1, recorded in the 200-800 nm wavelength regions. Mg doped $BiPo_4$ showed absorption on two peaks at wavelength of 240nm and 680nm respectively. Magnesium doping frequently produces defects or modifies the crystal field, which greatly depending on the quantity of Mg dopants. It can cause changes in the absorption edge toward the ultraviolet region (blue shift) or the visible region (red shift). Many other factors, including

Spectrum of Engineering Sciences
SPECTRUM OF ENGINEERING SCIENCES
Online ISSN
3007-3138
Print ISSN
3007-312X

oxygen deficit, d-d transitions, impurity centers, particle size, lattice distortion ratio and surface roughness can also affect absorbance. Changes in energy band gap are observed as a result of Mg^{2+} ions being substituted in the Bi^{3+} sites or interstitial places. If a material is UV-active, its energy band gap usually lies between 3.5 and 4.0 eV. Depending on the doping concentration, band gap can decrease, which is normally seen in the 2.8–3.5 eV region (Swart & Kroon, 2019). This decrease in energy improves the photo catalytic capabilities by permitting absorption in the visible light spectrum. Magnesium doping improves absorption of visible light by changing the band gap and adding defect levels.

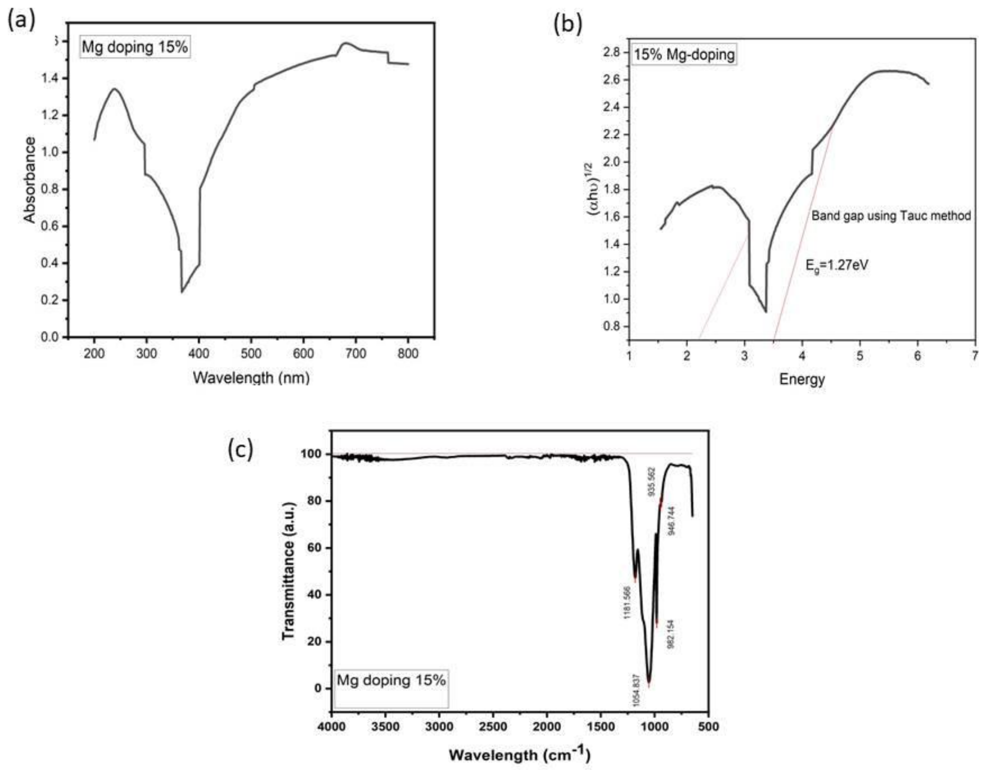

Fig.1 (a) Optical absorption spectra of Mg-doped $BiPO_4$. (b) Tauc plot for Mg-doped $BiPo_4$ (c) FTIR spectra of Mg-doped $BiPO_4$

Spectrum of Engineering Sciences
SPECTRUM OF ENGINEERING SCIENCES
Online ISSN
3007-3138
Print ISSN
3007-312X

Improvement in antibacterial efficacy can result from increased ROS production caused by enhanced light absorption. The sample's bandgap energy determined by plotting $(Ah\upsilon)^{1/\gamma}$ versus Energy (hυ). The energy bandgap value is obtained by linearly fitting the straight part of the curve on the hῦ axis, also known as the energy axis Wood and Tauc's equation provides the relationship between the incident photon energy (hυ) and the absorption coefficient (α).

$$(\alpha h\upsilon)^{1/\gamma} = A(h\upsilon - E_g)$$

Key factors in this formula are h (Planck's constant), v (photon frequency), E_g (optical bandgap energy), and A (constant) which are used to estimate the absorption coefficient (α) for nanoparticles. The γ factor, which determines the electron transition type, takes on a value of 1/2 or 2 for direct and indirect transition bandgap. By the plotting the value of $(\alpha h\upsilon)^{1/\gamma}$ with hυ and then extrapolating in the linear area over the energy axis in the associated graph, the optical band gap energy is computed using the Tauc's plot. An electron and a photon interacting with one another is a crucial aspect of direct transition. On the other hand, a three-particle interaction (photon, electron, and phonon) defines the essential characteristic of an indirect transition to maintain momentum conservation. The band gap spectra and energy values are shown in Figure 1(b). The bandgap energy is 1.27eV for 15% Mg-doped $BiPo_4$ nanoparticles. Due to the quantum size effect, Mg-doped $BiPo_4$ has large band gap then the Bulk $BiPo_4$. When the photon energy equals or surpasses the bandgap, electrons are excited from the valence band to the conduction band. In Mg-doped $BiPO_4$, the bandgap may shift because of particle confinement (larger bandgap) in nanostructures, defect states (smaller bandgap)

Spectrum of Engineering Sciences
SPECTRUM OF ENGINEERING SCIENCES
Online ISSN
3007-3138
Print ISSN
3007-312X

in bulk, or increased Mg doping concentrations. Under indoor or solar illumination, Mg-doped $BiPO_4$ exhibits improved absorption of visible light, which facilitates the photocatalytic production of reactive oxygen species (ROS) (Barone et al., 2014).

The energy transfer mechanism for magnesium (Mg)-doped bismuth phosphate ($BiPO_4$) primarily involves electronic transitions and charge-carrier dynamics that enhance its photocatalytic and functional properties. Mg-doped $BiPO_4$ produces electron-hole pairs (e^- in the conduction band and h^+ in the valence band) when it absorbs photons in the presence of light. By stabilizing the charges, magnesium ions function as charge traps, lowering the rate at which electron-hole pairs recombine. Magnesium ions prolong the lifespan of electrons and holes by improving the separation of charge carriers. By changing the surface characteristics of $BiPO_4$, magnesium doping increases the number of active sites available for the generation of ROS. Higher ROS concentrations brought on by the presence of magnesium ions boost the material's ability to inactivate microorganisms. Mg^{2+} ions replace Bi^{3+} ions in the lattice, causing lattice distortions that suppress the recombination of photogenerated electron-hole pairs.

The Mg doping increases the availability of charge carriers, ensuring their availability for subsequent reactions. Electrons in the valence band (VB) of $BiPO_4$ absorb photon energy and transition to the conduction band (CB), leaving behind holes in the VB. The Mg ions act as energy-level modifiers, improving the material's response to visible light (Choudhury & Choudhury, 2014). FTIR peaks are the strongest and most prominent as shown in Fig. 1(c). The asymmetry arises because the P atom is bonded to one or more oxygen atoms in the tetrahedral structure. Strong peaks

Spectrum of Engineering Sciences
SPECTRUM OF ENGINEERING SCIENCES
Online ISSN
3007-3138
Print ISSN
3007-312X

between 900 cm^{-1} and 1200 cm^{-1} are associated with the asymmetric and symmetric stretching vibrations of the PO_4^{3-} group. The shifts in vibrational modes of PO_4^{3-} and Bi-O bonds confirm structural modifications caused by Mg incorporation. Increased intensity of -OH peaks indicates better surface interaction, contributing to enhanced photocatalytic and antimicrobial performance. Despite doping, the presence of characteristic PO_4^{3-} and Bi-O peaks ensures that the fundamental $BiPO_4$ structure remains intact. Figure 1(C) shows the FTIR spectra of Mg-doped $BiPo_4$. Peaks appeared at 935, 946, 982, 1054 and 1181cm^{-1}. Bonding between these ranges are O-H stretching, Bi-S, and Asymmetrical C-F stretching (Kumar, Ratnakaram, et al., 2022).

Antimicrobial and Antifungal Activity

The antimicrobial activity of mg-doped bismuth phosphate's sample was studied against bacteria S. aureus and E. coli. The results shown in the Fig. revealed that, inhibition effect of sample containing mg-doped $BiPO_4$ against Gram positive and Gram negative bacteria is higher than others. The antimicrobial activity was evaluated by using the modified Disc. diffusion method. Filter paper discs soaked with mg-doped $BiPO_4$ nanoparticle suspension are placed on agar plates inoculated with microorganisms. Incubation and zone measurement follow. The results of antimicrobial screening reveal that by adding reactive sites and changing the surface charge, the magnesium doping improves the material's antibacterial activity and promotes oxidative stress by generating reactive oxygen species and rupturing bacterial membranes (Afeltra & Verweij, 2003). When compared to undoped bismuth phosphate, 15% Mg doping exhibits the greatest improvement, with larger zones of inhibition. According to this,

Spectrum of Engineering Sciences
SPECTRUM OF ENGINEERING SCIENCES
Online ISSN
3007-3138
Print ISSN
3007-312X

magnesium doping enhances the antibacterial qualities and has a synergistic impact, making magnesium-doped bismuth phosphate an effective substance for fighting microbial diseases. "The nanoparticles showed a stronger antimicrobial effect against *E. coli* compared to *Bacillus*, as evidenced by larger zones of inhibition (2.4cm vs. 1.8cm at 100 μg/mL).

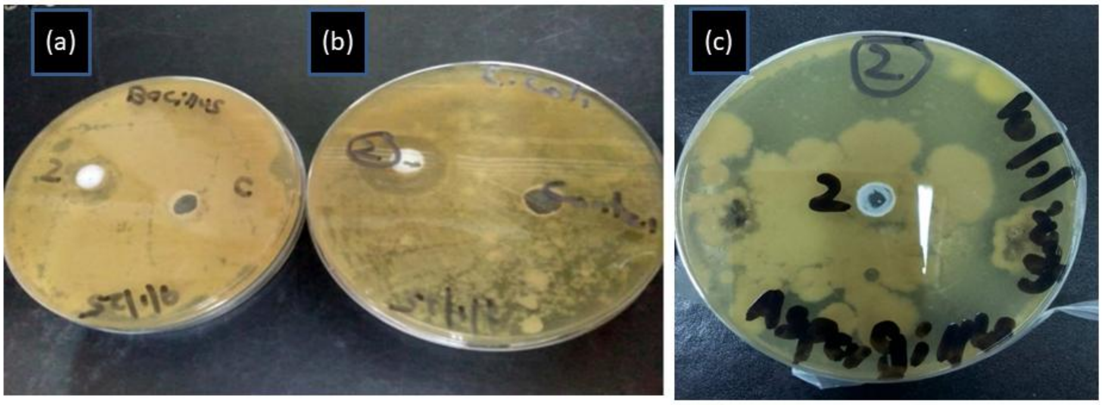

Figure 2 (a)Antimicrobial activity of mg-doped $BiPO_4$ E.coli (b) Antimicrobial activity of mg-doped $BiPO_4$ Bacillus) (c) antifungal activity

In recent studies on NP's as potential fungal disinfectants in different environments and provides information on the mechanisms of inactivation of these products by fungi. The antifungal activity of Mg-doped bismuth phosphate demonstrates notable efficacy against fungal strains, with enhanced inhibition. Among different doping levels, 15% Mg doping shows the highest antifungal activity, as evidenced by larger zones of inhibition and reduced fungal growth. Significant fungal growth suppression is revealed by the disc diffusion technique evaluation of Mg-doped bismuth phosphate's antifungal efficacy, especially at optimal doping doses. The efficacy of the material to prevent fungal growth is demonstrated by the discs impregnated with Mg-doped

Spectrum of Engineering Sciences
SPECTRUM OF ENGINEERING SCIENCES
Online ISSN
3007-3138
Print ISSN
3007-312X

bismuth phosphate, which show distinct zones of inhibition against tested fungal strains (Quiroga et al., 2001). Sample concentration was 10µg/ml and Aspergillosis (fungal strain) was used. Mg doped $BiPO_4$ nanoparticles inhibit growth of Aspergillosis fungus.

Conclusion and Future Prospective

Magnesium (Mg)-doped bismuth phosphate ($BiPO_4$) has emerged as a promising material due to its enhanced structural, optical, and catalytic properties compared to undoped $BiPO_4$. The incorporation of Mg ions into the $BiPO_4$ lattice induces structural modifications, such as improved crystallinity, altered bandgap, and enhanced surface area. These changes contribute to significant improvements in photocatalytic efficiency for applications like pollutant degradation, water splitting, and energy conversion. Mg-doping also stabilizes the material under harsh environmental conditions, making it a strong candidate for long-term industrial applications. Research can explore Mg-doped $BiPO_4$'s potential in advanced antimicrobials and fungal activities applications. A deeper understanding of the mechanisms driving Mg-induced enhancements in $BiPO_4$'s properties is essential. The material's potential for real-world applications in wastewater treatment, air purification, and energy harvesting systems should be investigated further, focusing on scalability and cost-efficiency.

References

Afeltra, J., & Verweij, P. (2003). Antifungal activity of nonantifungal drugs. *European Journal of Clinical Microbiology and Infectious Diseases*, *22*, 397-407.

Asghari, F., Jahanshiri, Z., Imani, M., Shams-Ghahfarokhi, M., & Razzaghi-Abyaneh, M. (2016). Antifungal nanomaterials:

Spectrum of Engineering Sciences

SPECTRUM OF ENGINEERING SCIENCES

Online ISSN

3007-3138

Print ISSN

3007-312X

synthesis, properties, and applications. In *Nanobiomaterials in antimicrobial therapy* (pp. 343-383). Elsevier.

Ashfaq, M. H., Imran, M., Haider, A., Shahzadi, A., Mustajab, M., Ul-Hamid, A., Nabgan, W., Medina, F., & Ikram, M. (2023). Antimicrobial potential and rhodamine B dye degradation using graphitic carbon nitride and polyvinylpyrrolidone doped bismuth tungstate supported with in silico molecular docking studies. *Scientific Reports*, *13*(1), 17847.

Bakht, J., Islam, A., Ali, H., Tayyab, M., & Shafi, M. (2011). Antimicrobial potentials of Eclipta alba by disc diffusion method. *African Journal of Biotechnology*, *10*(39), 7658-7667.

Barone, P., Stranges, F., Barberio, M., Renzelli, D., Bonanno, A., & Xu, F. (2014). Study of band gap of silver nanoparticles—Titanium dioxide nanocomposites. *Journal of Chemistry*, *2014*(1), 589707.

Biemer, J. J. (1973). Antimicrobial susceptibility testing by the Kirby-Bauer disc diffusion method. *Annals of Clinical & Laboratory Science*, *3*(2), 135-140.

Choudhury, B., & Choudhury, A. (2014). Oxygen defect dependent variation of band gap, Urbach energy and luminescence property of anatase, anatase–rutile mixed phase and of rutile phases of TiO2 nanoparticles. *Physica E: Low-Dimensional Systems and Nanostructures*, *56*, 364-371.

Damodaraiah, S., Prasad, V. R., Babu, S., & Ratnakaram, Y. (2017). Structural and luminescence properties of Dy3+ doped bismuth phosphate glasses for greenish yellow light applications. *Optical Materials*, *67*, 14-24.

Díez-Pascual, A. M. (2018). Antibacterial activity of nanomaterials. In (Vol. 8, pp. 359): MDPI.

Spectrum of Engineering Sciences
SPECTRUM OF ENGINEERING SCIENCES
Online ISSN
3007-3138
Print ISSN
3007-312X

Ianăși, C., Nemeş, N. S., Pascu, B., Lazău, R., Negrea, A., Negrea, P., Duteanu, N., Ciopec, M., Plocek, J., & Alexandru, P. (2023). Synthesis, Characterization and Antimicrobial Activity of Multiple Morphologies of Gold/Platinum Doped Bismuth Oxide Nanostructures. *International Journal of Molecular Sciences*, *24*(17), 13173.

Kumar, M., Ratnakaram, Y., Vijayalakshmi, R., & Raman, T. R. (2022). Probing into structural and spectroscopic properties of Dy3+ doped and Eu3+/Dy3+ co-doped bismuth phosphate (BiPO4) glass ceramics with different modifier fluorides. *Journal of Luminescence*, *245*, 118786.

Kumar, M., Vijayalakshmi, R., & Ratnakaram, Y. (2022). Investigation of structural and optical properties of Pr3+ doped and Pr3+/Dy3+ co-doped multicomponent bismuth phosphate glasses for visible light applications. *Journal of Molecular Structure*, *1265*, 133333.

Lin, D.-J., Tsai, M.-T., Shieh, T.-M., Huang, H.-L., Hsu, J.-T., Ko, Y.-C., & Fuh, L.-J. (2013). In vitro antibacterial activity and cytocompatibility of bismuth doped micro-arc oxidized titanium. *Journal of biomaterials applications*, *27*(5), 553-563.

Meng, T., Cai, S., Ling, L., Zuo, Y., Tian, H., Zhang, H., Zhang, H., & Xu, G. (2023). A wettability-transformable superhydrophobic composite coating of hydroxyapatite/bismuth sulfide/lauric acid on AZ31B Mg alloy with dual-function of antibacterial and osteogenic properties. *Ceramics International*, *49*(15), 25706-25715.

Murimadugula, S., Prasad, A., Lakshmi, A. M., Kumari, S., Rao, P. V., Raju, G. N., Kumari, K., Özcan, M., Madaboosi, N., & Prasad, P. S. (2024). Biomimetic Bi3+ substituted borate bioactive glasses

Spectrum of Engineering Sciences
Online ISSN
3007-3138
Print ISSN
3007-312X
SPECTRUM OF ENGINEERING SCIENCES

for bone tissue engineering via enhanced biological and antimicrobial activity. *Surfaces and Interfaces*, *51*, 104697.

Nagay, B. E., Dini, C., Cordeiro, J. M., Ricomini-Filho, A. P., De Avila, E. D., Rangel, E. C., Da Cruz, N. C., & Barao, V. A. (2019). Visible-light-induced photocatalytic and antibacterial activity of TiO2 codoped with nitrogen and bismuth: new perspectives to control implant-biofilm-related diseases. *ACS applied materials & interfaces*, *11*(20), 18186-18202.

Niemirowicz, K., Durnaś, B., Piktel, E., & Bucki, R. (2017). Development of antifungal therapies using nanomaterials. *Nanomedicine*, *12*(15), 1891-1905.

Pancotti, A., de Barros Souza, M. V., Santos Abreu, A., Rodrigues Rezende, S., Lázaro Moreli, M., Uceda Otero, E., Landers, R., Soares, R., & Wang, J. (2024). Evaluation of antibacterial activity of bismuth ferrites nanoparticles in the inhibition of E. coli and S. aureus bacteria. *Chemistry & Biodiversity*, e202402048.

Quiroga, E. N., Sampietro, A. R., & Vattuone, M. A. (2001). Screening antifungal activities of selected medicinal plants. *Journal of ethnopharmacology*, *74*(1), 89-96.

Swart, H., & Kroon, R. (2019). Ultraviolet and visible luminescence from bismuth doped materials. *Optical Materials: X*, *2*, 100025.

Wang, X., Liu, X., Chen, J., Han, H., & Yuan, Z. (2014). Evaluation and mechanism of antifungal effects of carbon nanomaterials in controlling plant fungal pathogen. *Carbon*, *68*, 798-806.